Nucl. Fusion **47** (2007) S718–S726 doi:10.1088/0029-5515/47/10/S19

Experimental progress on zonal flow physics in toroidal plasmas

A. Fujisawa[1], T. Ido[1], A. Shimizu[1], S. Okamura[1], K. Matsuoka[1], H. Iguchi[1], Y. Hamada[1], H. Nakano[1], S. Ohshima[1], K. Itoh[1], K. Hoshino[2], K. Shinohara[2], Y. Miura[2], Y. Nagashima[3], S.-I. Itoh[3], M. Shats[4], H. Xia[4], J.Q. Dong[5], L.W. Yan[5], K.J. Zhao[5], G.D. Conway[6], U. Stroth[7], A.V. Melnikov[8], L.G. Eliseev[8], S.E. Lysenko[8], S.V. Perfilov[8], C. Hidalgo[9], G.R. Tynan[10], C. Holland[10], P.H. Diamond[10], G.R. McKee[11], R.J. Fonck[11], D.K. Gupta[11] and P.M. Schoch[12]

[1] National Institute for Fusion Science, Oroshi-cho, Toki 509-5292, Japan
[2] Naka Fusion Institute, Japan Atomic Energy Agency, Naka-machi, Naka-gun, Ibaraki 311-0193, Japan
[3] Research Institute for Applied Mechanics, Kyushu University, Kasuga 816-8580, Japan
[4] Plasma Research Laboratory, Research School of Physical Sciences and Engineering, Australian National University, Canberra, ACT 0200, Australia
[5] Southwestern Institute of Physics, Chengdu 610041, People's Republic of China
[6] Max-Planck-Institut fur Plasmaphysik, EURATOM-Association IPP, Garching D-85748, Germany
[7] Universitat Stuttgart, Institut fur Plasmaforschung, Pfaffenwaldring 31 Stuttgart 70569, Germany
[8] Nuclear Fusion Institute, RRC 'Kurchatov Institutef, 123182, Moscow, Russia
[9] Associacion Euratom-Ciemat para Fusion, Avenida Complutense 22, Madrid 28040, Spain
[10] University of California, San Diego, La Jolla, CA 92093, USA
[11] University of Wisconsin-Madison, 1500 Engineering Drive, Madison, Wisconsin 53706, USA
[12] Rensselaer Polytechnic Institute, Troy, New York 12180, USA

E-mail: fujisawa@nifs.ac.jp

Received 6 December 2006, accepted for publication 8 March 2007
Published 19 September 2007
Online at stacks.iop.org/NF/47/S718

Abstract
The present status of experiments on zonal flows in magnetic confinement experiments is examined. The innovative use of traditional and modern diagnostics has revealed unambiguously the existence of zonal flows, their spatio-temporal characteristics, their relationship to turbulence and their effects on confinement. In particular, a number of observations have been accumulated on the oscillatory branch of zonal flows, named geodesic acoustic modes, suggesting the necessity for theories to give their proper description. In addition to these basic properties of zonal flows, several new methods have elucidated the processes of zonal flow generation from turbulence. Further investigation of the relationship between zonal flows and confinement is strongly encouraged as cross-device activity including low temperature, toroidal and linear devices.

PACS numbers: 52.25.Fi, 52.25.Gj, 52.35.Ra, 52.55.−s

(Some figures in this article are in colour only in the electronic version)

1. Introduction

Drift-wave turbulence has been extensively studied for a long time to clarify the anomalous transport governing toroidal plasma confinement [1, 2]. The discovery of H-mode [3] highlighted the effect of macroscopic flow or radial electric field on turbulence, and the self-organization process of flows and turbulence. Recently, theories and simulations have predicted another important player in plasma transport, i.e. zonal flows-mesoscale structure of radial electric field [4, 5]. In this new framework that the theories proposed, zonal flows should exist in toroidal plamas and should play an important

role in controlling the transport level of the plasma through nonlinear interaction with drift-wave turbulence. It has also been confirmed in simulations that the treatment of zonal flows should affect the confinement property of toroidal plasmas.

The experimental confirmation of zonal flows has been an urgent and important issue in order to give reliable predictions of the performance of toroidal plasma devices including burning ones in the next generation, such as ITER. Actually, elaborate experimental trials have been made to detect zonal flows, using advanced diagnostics and analysing techniques, in a number of toroidal and linear devices in spite of the difficulty of capturing the meso- and microscale structures in plasmas. Recent experiments on zonal flows and turbulence have made great progress, thanks to worldwide efforts, in confirming the existence of zonal flows and in proving their interaction with turbulence.

Presently, the experimental observations have been accumulated to a sufficient extent to be systematized to provide answers regarding the fundamental aspects of the physics of zonal flows. This paper aims at providing a brief overview of the experimental achievements in zonal flows and turbulence, and at demonstrating the experimental validity of the new theoretical paradigm; i.e. plasma turbulence should be regarded as a system of zonal flows and drift-wave turbulence. The basic features of zonal flows in structure and dynamics, dependences of zonal flow characteristics on plasma parameters and magnetic configurations and the quantification of their impacts on turbulence and transport are discussed.

2. Experimental physics of zonal flows

Zonal flows are fluctuations that are linearly stable but nonlinearly driven by turbulence. Zonal flows are characterized by their symmetric nature around the magnetic axis, that is, $m = n = 0$ structure in the poloidal and toroidal directions, and have a rapidly varying structure with a finite wavelength in the radial direction. The symmetric characteristics result in no cross-field transport associated with zonal flows. The experimental identification of zonal flows requires two major issues: to find fluctuating structures that satisfy $m = n = 0$ and $k_r \neq 0$, and to confirm that the structures are generated by background turbulence. Two kinds of zonal flows have been expected in toroidal plasmas: stationary zonal flows and geodesic acoustic modes (GAMs) [6]. Stationary zonal flows fluctuate at quite low frequencies, while the GAM is an oscillatory branch. The $m = 1$ asymmetry of the toroidal plasma is the driving force of the GAM. The density fluctuation having the $m = 1$ structure is expected to be accompanied by the GAM, while no significant density fluctuation is expected for stationary zonal flows. Theories predict that the GAM frequency should be expressed as $f \propto c_s/R$, where c_s and R represent the sound wave velocity and the major radius of the device, respectively.

In experiments, zonal flows can be detected by direct measurements of plasma flow or radial electric field. The Langmuir probes are the simplest method to detect zonal flows through electrostatic potential measurement [7, 8], although the applicable region is limited to the plasma edge in modern high temperature plasmas. The heavy ion beam probe (HIBP) is capable of detecting electrostatic potential inside the high temperature core of the plasma [9–13]. Besides, other methods to detect the flow indirectly have been developed recently, such as beam emission spectroscopy (BES) with the time-delay-estimation (TDE) technique [14] and Doppler reflectometry (DR) [15]. The experimental results related to zonal flows that have been obtained to date are summarized in table 1. As shown in table 1, the zonal flow experiments take place over a wide range of plasma parameters in a variety of devices. In a physical sense, dimensionless studies extensively performed in TJ-K contribute to a systematic physical understanding of plasma turbulence by providing a bridge between plasmas in quite different ranges of parameters, i.e. large fusion-oriented research and university laboratory studies for fundamental plasma study [16].

3. Fundamental observations on zonal flows

3.1. Fluctuation spectra

A fundamental method for studying a system of zonal flows and drift-wave turbulence is to obtain the fluctuation spectrum. Figure 1 shows examples of frequency spectra in CHS, T-10, TEXT and JFT-2M (measured with HIBPs), together with those in ASDEX-U (measured with DR) and from DIII-D (measured with BES). One common feature of the spectra in figure 1 is, obviously, the existence of solitary peaks, which are conjectured as GAMs. At present, many of the fluctuation spectra measurements aimed at zonal flow identification have been performed in the frequency domain. Complementarily, a few wavenumber spectra have been obtained using Langmuir probe arrays in rather low temperature devices: CSDX [17], H1-heliac [18] and TJ-K [19].

The correlation property of fluctuations in the observable frequency range has been measured with dual HIBPs in CHS. The fluctuation spectrum can be divided roughly into three characteristic frequency regions: (I) stationary zonal flow region in the low frequency regime (less than ∼2.5 kHz) to show a long-distance correlation, (II) sharp peaks conjectured as GAMs to show a long-distance correlation (from 30 to 50 kHz) and (III) broad-band turbulence (around 50 kHz) with short correlation length. This classification could be applied to the spectra of the other toroidal devices.

3.2. Stationary zonal flows

Identification of stationary zonal flows essentially requires the multipoint detection of flow or radial electric field in order to prove its symmetric nature. Several methods without multipoint detection have also been invented to detect stationary zonal flows; for example, the autocorrelation width technique applied in the CASTOR tokamak [20] and the detection technique of Doppler frequency modulation due to zonal flow in the Colombia Linear Machine (CLM) [21]. A pioneering work to search for stationary zonal flows was performed in the HT-7 tokamak using a forked Langmuir probe, reporting the existence of a long-poloidal wavelength $E \times B$ time varying flow to satisfy the requirement of zonal flows [8].

Identification of zonal flows in the high temperature core succeeded in CHS using twin HIBPs located at two different toroidal positions separated by 90° [10]. The measurement

Table 1. The present status of experiments on zonal flows.

Device	Diagnostics	Aspects of study (reference number)
ASDEX-U $R(m)/a(m) = 1.65/0.5$	Doppler reflectometry	– GAM study (symmetry, dispersion, etc) [15]
CASTOR $R(m)/a(m) = 0.4/0.085$	Langmuir probes	– Development of detection method of ZFs [20]
CHS $R(m)/a(m) = 1.0/0.2$	HIBPs	– Study of ZFs and GAM [10, 29] – Coupling with turbulence [46] – Effects on transport [47]
CLD $L(m)/a(m) = 1.6/0.03$	Langmuir probes	– Development of detection method of ZFs [21]
CSDX (linear machine) $L/a(m) = 3./0.045$	Langmuir probes	– Wavenumber spectrum [40] – Reynolds stress measurement [17]
DIII-D $R(m)/a(m) = 1.7/0.6$	Beam emission spectroscopy Langmuir probe	– GAM study (symmetry, dispersion) [14, 27] – Study of ZFs [22] – Bicoherence before and after LH transition [39]
H1 $R(m)/a(m) = 1.0/0.2$	Triple probe arrays radially and poloidally aligned	– GAM study (symmetry, coupling, basic feature, etc) [7, 28] – Coupling and energy transfer [18, 45] – Effect on transport [48]
HL-2A $R(m)/a(m) = 1.65/0.4$	Three step Langmuir probe arrays	– GAM study (symmetry, basic featre, coupling) [24]
HT-6M $R(m)/a(m) = 0.65/0.19$	Triple and Mach probes	– Reynolds stress during H-mode transition [35]
HT-7 $R(m)/a(m) = 1.22/0.27$	Forked Langmuir probe	– Study of ZFs [8]
JFT-2M $R(m)/a(m) = 1.3/0.3$	HIBP Reciprocating Langmuir probes	– GAM study (symmetry, spatial structure, basic feature, etc) [12] – Bicoherence analysis on GAM and turbulence [23, 41]
JIPPT-IIU $R(m)/a(m) = 0.93/0.23$	HIBP	– GAM study (symmetry, basic feature, etc) [11] – Streamer study [49]
T-10 $R(m)/a(m) = 1.5/0.3$	HIBP , Correlation reflectometer and Langmuir probes	– GAM study (symmetry, dispersion, spatial structure, density fluctuation) [13, 50]
TEXTOR $R(m)/a(m) = 1.75/0.47$	Reflectometer	– Symmetry and structure of GAM in density fluctuation [25]
TEXT-U $R(m)/a(m) = 1.0/0.27$	HIBP	– GAM study [9]
TJ-II $R(m)/a(m) = 1.5/0.22$	Langmuir probes	– Reynolds stress at the plasma edge [33, 34, 37]
TJ-K $R(m)/a(m) = 0.6/0.1$	Probe arrays	– Dimensionless analysis of turbulence [16, 19]

system confirms that the electric field fluctuations ranging from ∼0.5 to ∼1 kHz should have toroidal symmetry of $n = 0$ with finite radial wavenumbers. Figure 2 shows the radial correlation function between the electric field at $r = 12$ cm and the other location varying from 10 to 14 cm, showing the spatio-temporal pattern of the stationary zonal flows. The observation shows the zonal flows with a finite radial wavelength of ∼1 cm do exist, and the zonal flow loses the memory of its structure in ∼2 ms. Recently, the BES experiments in DIII-D have provided supportive evidence for the existence of low frequency fluctuation with $m = 0$ symmetry, which is conjectured as the stationary zonal flow [22].

3.3. GAMs

It could be easier to capture the signatures of GAMs than the stationary zonal flows owing to the former's oscillatory nature. Following the GAM identification in the H1-heliac [7], solitary peaks have been found in the fluctuation spectra of a number of toroidal plasmas (see figure 1). The multi-channel property of the HIBP is used to obtain the poloidal mode number of the oscillation. In JIPPT-IIU [11], JFT-2M [12] and T-10 [13], the poloidal mode numbers of the oscillations are inferred as $m \sim 0$, proving that the modes should be GAMs (see table 1). In DIII-D, multipoint detection also proves that the observed solitary mode should have an $m = 0$ poloidal mode structure [14]. The other multi-channel array Langmuir probes in H1 [7] and JFT-2M [23] also show the poloidally symmetric structure of the mode ($m = 0$). Recently, in the Chinese device, HL-2A, the complete symmetric characteristics of $m = n = 0$ have been confirmed using probe measurements in the edge of Ohmic discharges [24]. Moreover, the details of density fluctuations accompanying GAMs have been reported in measurements using a correlation reflectometer in TEXTOR [25].

The variability of observation points of diagnostics can estimate the radial localization or extent of the modes in

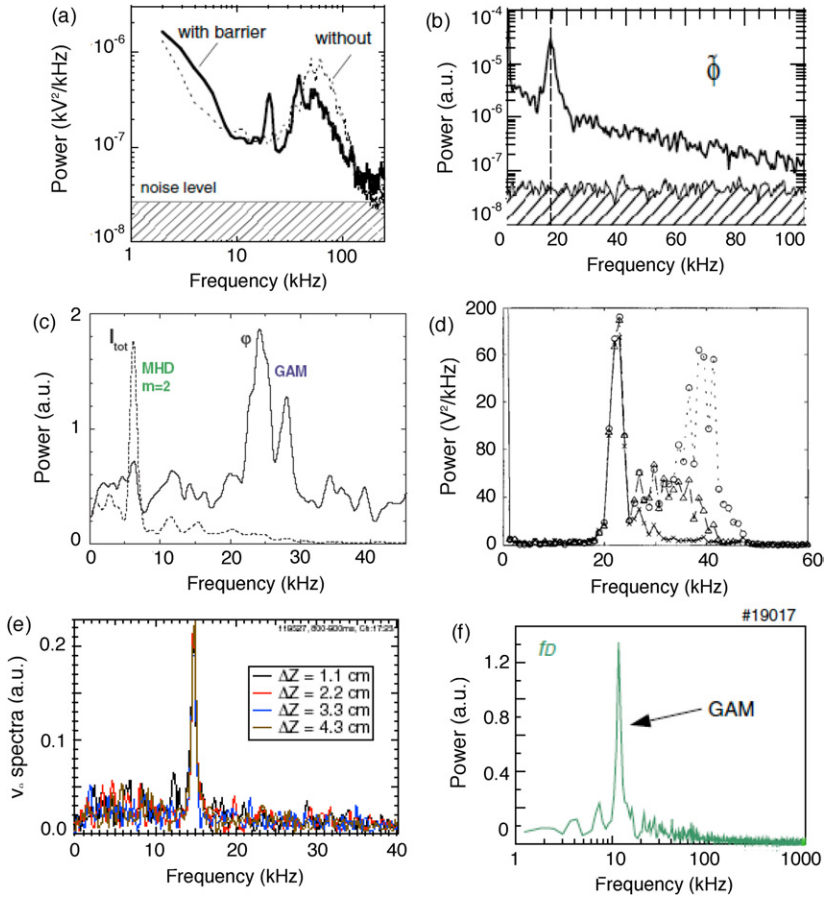

Figure 1. Potential fluctuation spectra measured with HIBP. (*a*) Electric field fluctuation in CHS [46]. (*b*) Potential fluctuation spectra in JFT-2M. The hatched area means the noise level [12]. (*c*) Potential and density fluctuation spectra in T-10 [13]. The detected beam current of the HIBP system, I_{rmtot}, reflects the local density fluctuation. (*d*) Potential fluctuation spectra in TEXT -U for three different locations. The crosses, diamonds and circles correspond to $\rho = 0.85$, $\rho = 0.76$ and $\rho = 0.69$, respectively [9]. (*e*) Velocity fluctuation spectra measured with BES in DIII-D [14]. (*f*) Spectrum of Doppler frequency measured with DR in ASDEX-U [15].

JFT-2M (HIBP), T-10 (HIBP), CHS (HIBP), DIII-D (BES) and ASDEX-U (DR). Commonly, the modes (GAMs) are found to be localized in a rather narrow radial extent of a few cm for these cases. The observation in JFT-2M reported the eigenmode characteristics of the GAM, that is, the mode is localized in ∼5 cm inside the separatrix without a change in frequency, while the electron temperature increases significantly towards the core (see figure 3). In addition, the outward propagation characteristics of the GAM are deduced, as shown in figure 3 [26].

The experimental GAM frequency has been compared with theoretical expectation in a number of devices. In every trial, it has been confirmed that the GAM frequency should be proportional to the sound velocity although a somewhat different coefficient is found in different conditions even in the same device. In ASDEX-U, the frequency dependence on the geometrical factors is investigated, such as the safety factor, q, and the ellipticity, κ. The results suggest strong inverse and weak non-inverse dependences on κ and q, respectively [15]. Figure 4 shows the observed GAM frequencies in different devices as a function of c_s/R.

In DIII-D, the dependence of GAM amplitude on q was investigated [27]. It is found that the GAM amplitude tends to increase as the q-value increases, while the GAM is almost undetectable when $q_{95} > 8$. The positive dependence of the GAM amplitude on the q-value suggests that the process of Landau damping should be important to determine the GAM level. In comparison, the amplitudes of GAMs are much stronger in tokamaks than in helical devices (CHS and H1). Analysis in H1-heliac indicates that the larger inhomogeneity of magnetic field configuration in helical plasmas is the cause of the small fraction of the zonal flow component [28].

It is found in the ECR-heated plasma of CHS that two different modes conjectured as GAMs coexist in a quite narrow range of frequency (actually at 16 and 18 kHz). The two modes show quite different radial distributions, and the features indicate eigenmode characteristics [29]. In the T-10 and TEXTOR tokamaks, similarly to this CHS observation, multiple peaks called satellites are found to accompany the GAM peak [13,25]. These observations suggest that the GAM should have discrete frequencies, whose dependence obeys the theoretical expectation i.e. $f_{\mathrm{GAM}} \propto c_s/R$. In addition, the solitary peak is sharp but has a finite width to indicate the finite lifetimes of the GAMs. In fact, intermittent characteristics of GAMs have been reported in many devices, such as CHS, JFT-2M and T-10. In order to investigate the spatial structure of the GAMs and the temperature dependence of the GAM frequency, the suggested eigenmode characteristics and

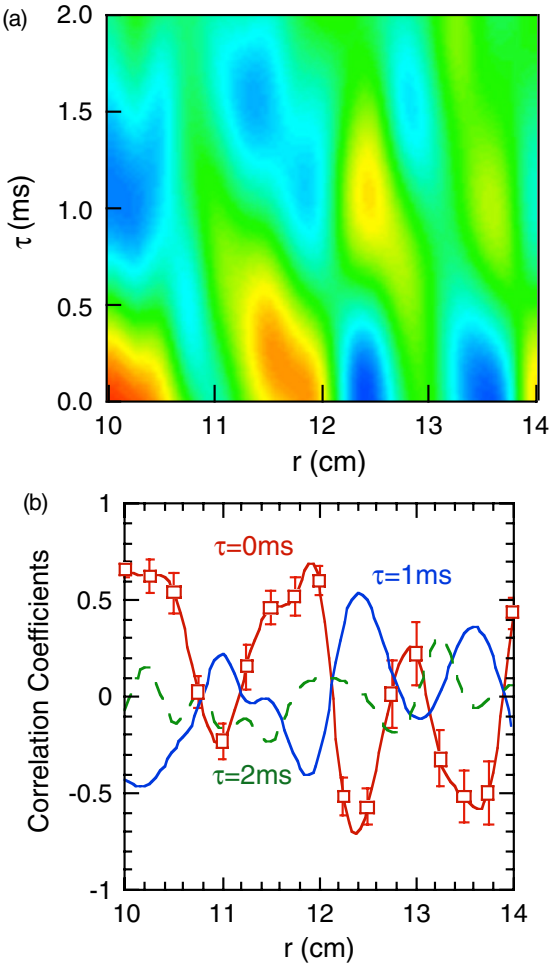

Figure 2. (*a*) Spatio-temporal structure of stationary zonal flows evaluated from the correlation function in CHS. (*b*) Spatial correlation with the time lag of $\tau = 0$, 1 and 2 ms.

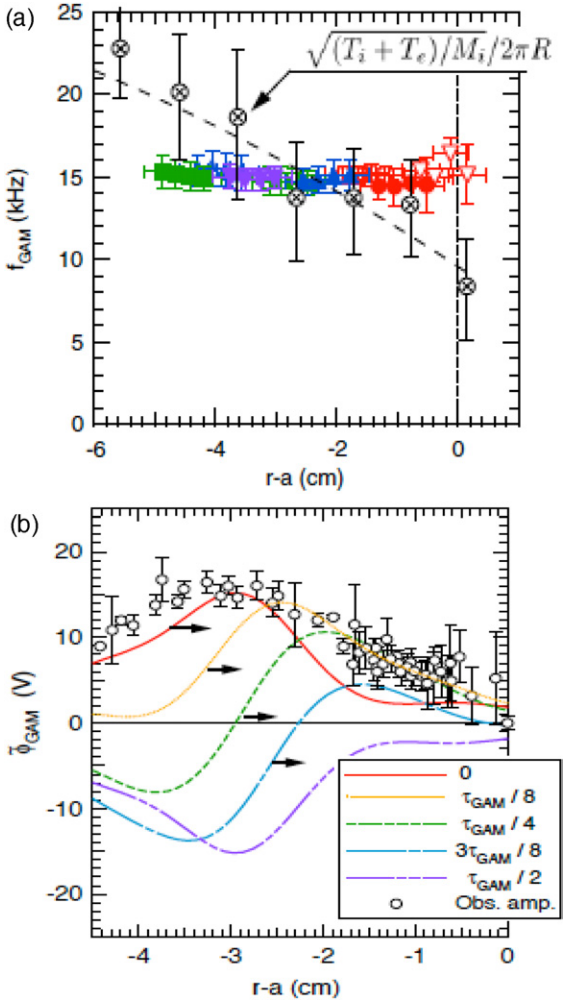

Figure 3. GAM structure in JFT-2M [12]. (*a*) GAM frequency as a function of radius. The circles show the GAM frequency expected from the ion temperature measured with charge exchange spectroscopy with an assumption of $T_e = T_i$. The dashed line indicates a fitting line. (*b*) The temporal change in the GAM structure that indicates outward propagation.

intermittent nature should be taken into account for future analysis. New theories of GAMs have been developed to describe eigenmode characteristics and radial localizations of GAMs for comparison with experimental data [30–32].

4. Nonlinear interaction between zonal flows and turbulence

4.1. Quantification of flow generation process by turbulence

It is considered that zonal flows should be generated by turbulence through three-wave couplings expressed by the $\langle v\nabla v\rangle$ nonlinearity (or the Reynolds stress term), similarly to the mean flow. The Reynolds stress has been directly evaluated in the edge regions of high temperature plasmas [33, 34] and low temperature plasma such as CDSX [17]. In particular, the Reynolds stress measurements at the edge of HT-6M suggested that the mean flow in the H-mode transition should be generated by turbulence [35], consistent with the Prey and Predator model [36]. Recent probe experiments in TJ-II have indicated that, in addition to the perpendicular component traditionally measured $\langle\tilde{v}_\perp\tilde{v}_r\rangle$, the parallel component $\langle\tilde{v}_\parallel\tilde{v}_r\rangle$ should play an important role in the energy transfer from turbulence to flows [37].

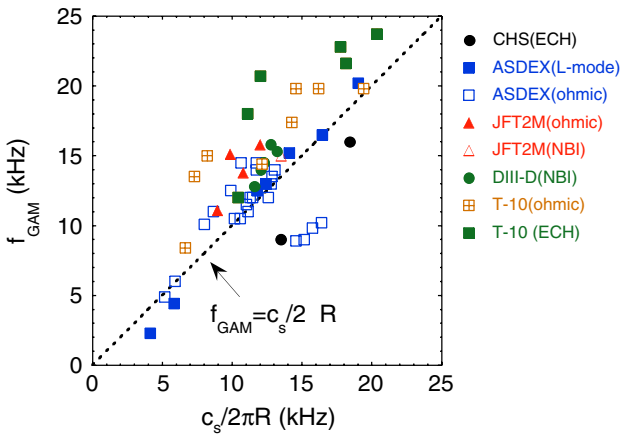

Figure 4. A comparison between the observed GAM frequency and theoretical prediction. Here, c_s and R are the ion sound velocity and the major radius, respectively.

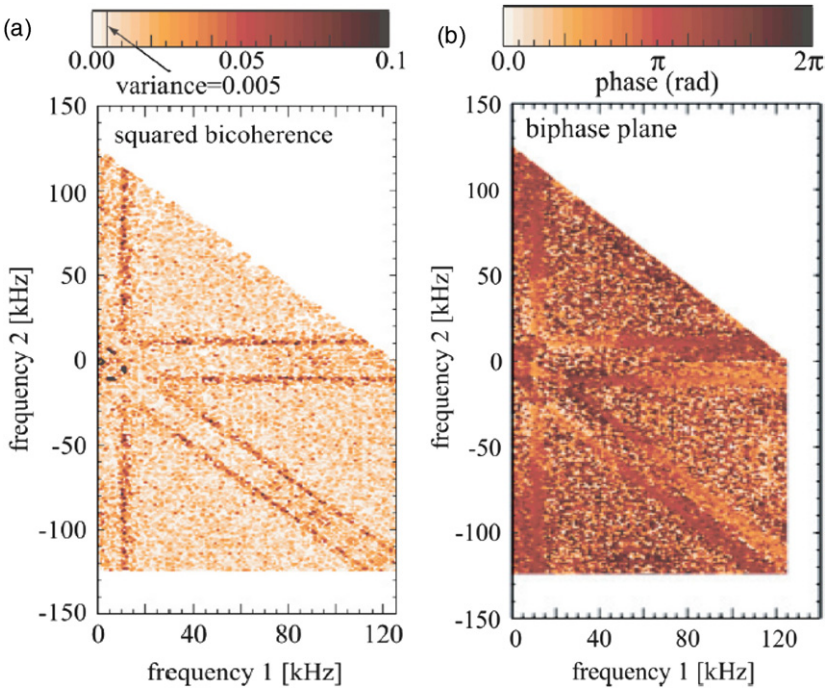

Figure 5. Bicoherence analysis to show the coupling between GAM and background turbulence in JFT-2M [23, 41]. (*a*) Bicoherence evaluated with potential fluctuation at the plasma edge and (*b*) corresponding biphase.

The strength of three-wave couplings can be qualified with bicoherence analysis [38]. The definition of bicoherence is $b_c = |\langle g^*_{f_3} g_{f_2} g_{f_1}\rangle|^2/(\langle|g_{f_3}|^2\rangle\langle|g_{f_2}g_{f_1}|^2\rangle)$, where g_{f_n} is the Fourier coefficient at a frequency f_n, and $f_1 + f_2 = f_3$ is satisfied, and $\langle\ \rangle$ represents the ensemble average. Therefore, bicoherence can measure the phase coherency between different frequency waves, and the bicoherence value becomes large if phase coherency between three waves f_1, f_2 and f_3 is high. An increase in bicoherence was found in the transient phase from the L- to the H-mode, which implies that an increase in the Reynolds stress results in the generation of a large mean flow in the H-mode [39].

The bicoherence analysis has been applied to prove the existence of couplings between turbulent waves in CSDX [40], H1-Heliac [7], HL-2A [24], HT-7 [8] and JFT-2M [41]. For example, the bicoherence diagrams in JFT-2M are shown in figure 5. In JFT-2M, bicoherence analysis was applied to potential fluctuations measured with a Langmuir probe at the plasma edge. Obviously, the lines of $f_1 + f_2 = \pm 10$ kHz in the diagram show a clear high level of coupling, and the biphase is constant on the lines. Therefore, the bicoherence clearly demonstrates the existence of the coupling between GAMs and turbulence and that the modulational instabilities should be associated with zonal flow generation [4]. A theoretical base is proposed to connect the obtained bicoherence value to the strength of three wave coupling [42].

4.2. Energy transfer between zonal flows and turbulence

Energy transfer between disparate-scale waves or fluctuations has been studied using nonlinear energy transfer [43] and autocorrelation analyses [44] in the H1-heliac. These analyses have shown evidence of inverse cascade in both frequency and wavenumber domains, and a difference in the energy transfer structure between the L- and the H-modes [17, 28, 45]. In a linear machine, CSDX, fluctuations with low poloidal wavenumbers, which are linearly stable, are found to develop as a turbulent state is realized with an increase in the magnetic field [16, 40]. This suggests that the turbulence energy is transferred nonlinearly from turbulence into zonal flows in the wavenumber domain.

Wavelet analysis reveals the temporal correlation between disparate-scale components of electric field fluctuations [46]. Figure 6 demonstrates the temporal evolutions of the wavelet powers of these three fluctuation regimes. Here, wavelet power is defined as an integral expressed as $q(f_1, f_2) = \int_{f_1}^{f_2} |W_f|^2\, \mathrm{d}f$ where W_f is the wavelet coefficient. It is obvious that the lower frequency regime close to a stationary zonal flow (here, $2.5 < f < 10$ kHz, called here zonal flows' tail) is anti-correlated with the power of the turbulence ($30 < f < 250$ kHz). On the other hand, the power of the GAM shows no significant correlation with those of the tail and the turbulence. Note that here the powers are normalized by the total power in order to remove the variation in the total fluctuation power, which may be associated with a change in bulk plasma parameters such as the pressure gradient. A recent study suggests that both the powers of the tail and of the turbulence are modulated by the zonal flow phase. Further investigation is necessary to elucidate the energy transfer between the fluctuation components; stationary zonal flow, tail, GAM and turbulence.

4.3. Role of zonal flows on transport and confinement

So far we have had a few experiments to demonstrate the effect of zonal flows on plasma transport and confinement. The HIBPs are able to estimate particle transport through simultaneous detection of density and potential fluctuations.

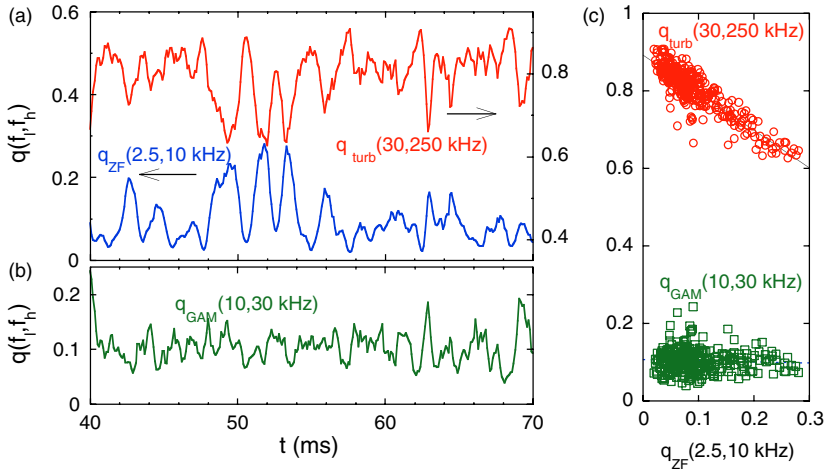

Figure 6. Wavelet power relationship between turbulence, GAM and ZF-tail fluctuation in CHS [46]. (*a*) The power of the tail shows anti-correlation with that of turbulence in time evolution and (*b*) no correlation with GAM. (*c*) Powers of turbulence and GAM as a function of that of the zonal flow tail.

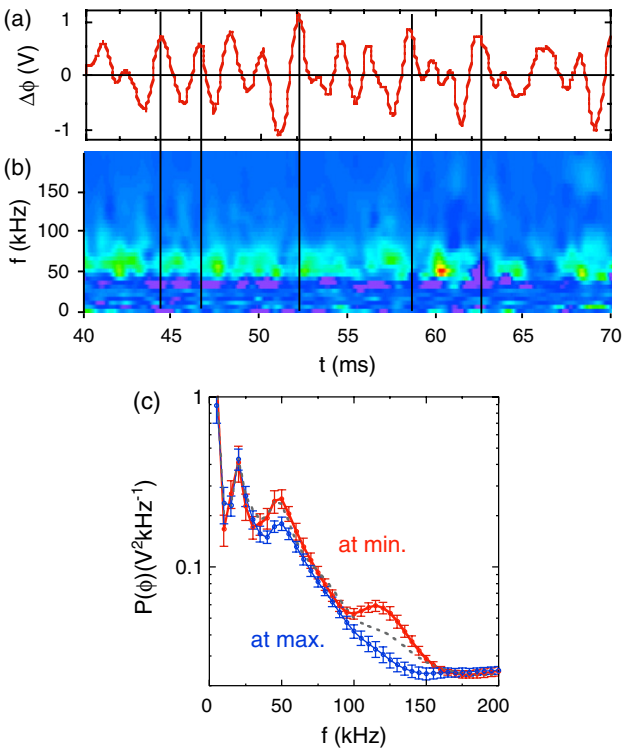

Figure 7. The modulation effect of stationary zonal flow on particle transport in CHS [47]. (*a*) Temporal evolution of stationary zonal flows and (*b*) an image plot of particle flux. (*c*) Conditional averages of potential fluctuation spectra in the time windows discriminated by the phase of zonal flow; i.e. maxima, zero and minima.

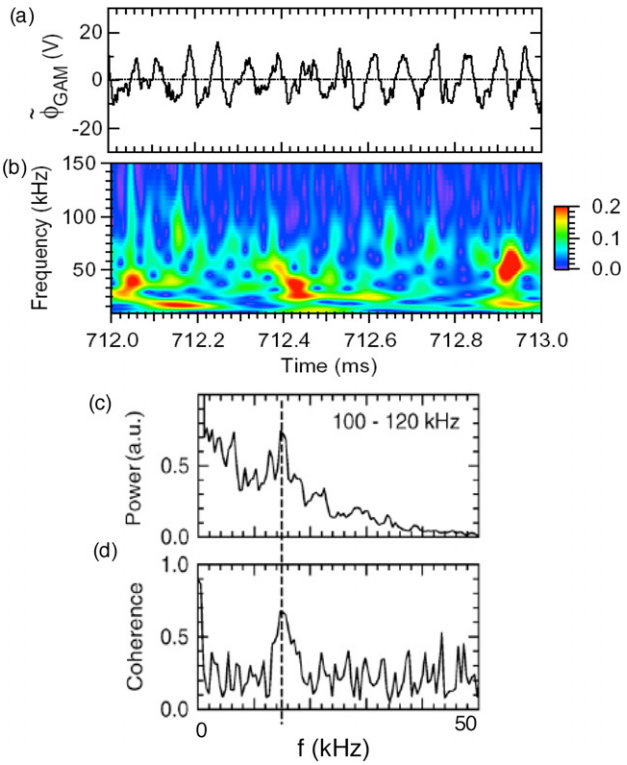

Figure 8. The modulation effect on turbulence in JFT-2M [26]. (*a*) Time evolution of potential at GAM frequency and (*b*) that of the normalized density fluctuation. (*c*) Power spectrum of the density fluctuation amplitude whose frequency ranges from 100 to 120 kHz and (*b*) its coherence with GAM fluctuations.

It is found by utilizing the advantage that the particle transport should be modulated by the zonal flow phase in CHS. Figure 7 shows the modulation effect of a stationary zonal flow on turbulence. Here, instantaneous fluctuation amplitudes of density and potential are evaluated using the Gabour's wavelet transformation, and fluctuation-driven particle flux was calculated [47]. In addition, a significant change in the potential fluctuation spectrum is deduced by taking a conditional average according to the zonal flow phases, maxima, minima and zero phases. Figure 7(*b*) demonstrates a clear difference in the fluctuation spectrum according to the zonal flow phase. However, one should be cautious regarding the fact that the measured potential fluctuations could contain electric field fluctuations along the probing beam orbit.

A similar analysis was performed in JFT-2M to study the relation between the GAM and turbulence [12, 26]. Figure 8 shows the temporal evolutions of the band-pass

filtered potential at the GAM frequency and of the wavelet spectrum of the density fluctuations. The density fluctuations appear to be modulated by the GAM frequency. Figure 8(*c*) shows the Fourier spectrum on the waveform of the wavelet power of the density fluctuation (see figure 8(*b*)) ranging from 100 to 120 kHz. Obviously, the Fourier spectrum indicates a sharp peak consistent with the GAM frequency. As a result, it is confirmed that the density fluctuations are modulated with the GAM evolution. A similar modulation of the turbulence amplitude with the GAM was suggested in the correlation reflectometer experiment in TEXTOR [25].

Several ways for the zonal flows to affect turbulence and the resultant transport are predicted, such as time-dependent electric field shearing and the energy transfer between them. It is found in the H1-heliac that the phase randomization of fluctuations due to zonal flow should be the major cause of a reduction in the turbulence driven transport [48]. Although the present experimental precision in the high temperature core cannot tell what mechanism is dominant for turbulence regulation in the high temperature plasmas, observations show the existence of significant coupling between zonal flows and turbulence.

5. Concluding remarks

The presented experimental results have confirmed, using many diagnostic techniques, that zonal flows really do exist in toroidal plasmas. The observations of zonal flows have accumulated to show spatial structures and dynamics, and a number of advanced analysis techniques, such as bicoherence, have been applied to show the coupling between zonal flows and turbulence. Particularly, it is a significant step forward for fusion to prove the existence of stationary zonal flows and their coupling with turbulence.

On the other hand, many observations of GAMs from worldwide devices have provided information on their basic features, such as the axisymmetric structure, the dispersion relation, the coupling with turbulence and the accompanying density fluctuation. Most of the observations agree well with the predictions of theory, for example, the essential dependence of the GAM frequency should obey the theoretical expectation, $f_{\mathrm{GAM}} \propto c_{\mathrm{s}}/R$. However, the observations of GAMs have provided several features to be clarified, such as their intermittent characteristics and eigenmode properties. GAMs have been found to be localized in a rather narrow regime of plasmas with a constant frequency with an eigenmode property, and the co-existence of multiple GAMs with discrete frequencies has been suggested. However, no theories are available to predict how the eigenmode having the observed frequency selectively grows in the real experimental situation.

Finally, the experimental observations to date have already demonstrated that zonal flows really do regulate the plasma turbulence and resultant transport. Therefore, this experimental fact supports the theoretical expectation that better confinement is achieved when the ratio of zonal flow to turbulence is larger, and indicates a future experimental direction to investigate under what conditions the zonal flow can grow by suppressing turbulence. The answer to this is a key to optimizing the magnetic configuration for confinement. Comparative works should be required amongst a wide variety of magnetic configurations and conditions to obtain the answer. Hence, worldwide cooperation should be necessary to clarify zonal flow physics and better confinement.

Acknowledgments

The first author (A.F.) devotes this work to Professor A. Iiyoshi for his 70th birthday. This work is partly supported by the Grants-in-Aid for Specially-Promoted Research (16002005) and Scientific Research (18360447). The Russian team is supported by grants NSh 2264.2006.2, RFBR 05-02-1706, INTAS 1000008-8046 and NWO-RFBR 047-016-015.

References

[1] Liewer P.C. 1985 *Nucl. Fusion* **25** 543
[2] Wootton A. *et al* 1990 *Phys. Fluids* B **2** 2879
[3] Wagner F. *et al* 1982 *Phys. Rev. Lett.* **49** 1408
[4] Diamond P.H., Itoh K., Itoh S.-I. and Hahm T.S. 2005 *Plasma Phys. Control. Fusion* **47** R35
[5] Rosenbluth M.N. and Hinton F.L. 1998 *Phys. Rev. Lett.* **80** 724
[6] Winsor N., Johnson J.L. and Dawson J.M. 1968 *Phys. Fluids* **11** 2448
[7] Shats M.G. *et al* 2002 *Phys. Rev. Lett.* **88** 045001
[8] Xu G.S., Wan B.N., Song M. and Li J. 2003 *Phys. Rev. Lett.* **91** 125001
[9] Schoch P.M. *et al* 2003 *Rev. Sci. Instrum.* **74** 1846
[10] Fujisawa A. *et al* 2004 *Phys. Rev. Lett.* **93** 165002
[11] Hamada Y. *et al* 2005 *Nucl. Fusion* **45** 81
[12] Ido T. *et al* 2006 *Nucl. Fusion* **46** 512
[13] Melnikov A.V. *et al* 2006 *Plasma Phys. Control. Fusion* **48** S87
[14] Mckee G.R. *et al* 2003 *Plasma Phys. Control. Fusion* **45** A477
[15] Conway G.D. *et al* 2005 *Plasma Phys. Control. Fusion* **47** 1165
[16] Lechte C., Neidner S. and Stroth U. 2002 *New J. Phys.* **4** 34
[17] Tynan G.R., Holland C, Yu J.H., James A., Nishijima D., Shimada M. and Taheri N. 2006 *Plasma Phys. Control. Fusion* **48** S51
[18] Shats M.G., Xia H. and Punzmann H. 2005 *Phys. Rev.* E **71** 046409
[19] Stroth U. *et al* 2004 *Phys. Plasmas* **11** 2558
[20] Bencze A. *et al* 2006 *Plasma Phys. Control. Fusion* **48** S137
[21] Sokolov V., Wei X., Sen A.K. and Avinash K. 2006 *Plasma Phys. Control. Fusion* **48** S111
[22] Gupta D.K., Fonck R.J., McKee G.R., Schlossberg D.J. and Shafer M.W. 2006 *Phys. Rev. Lett.* **97** 125002
[23] Nagashima Y. *et al* 2006 *Plasma Phys. Control. Fusion* **48** S1
[24] Zhao K.J. *et al* 2006 *Phys. Rev. Lett.* **96** 255004
[25] Krämer-Flecken A., Soldatov S., Koslowski H.R., Zimmermann O. and TEXTOR Team 2006 *Phys. Rev. Lett.* **97** 045006
[26] Ido T. *et al* 2006 *Plasma Phys. Control. Fusion* **48** S41
[27] McKee G.R. *et al* 2006 *Plasma Phys. Control. Fusion* **48** S123
[28] Shats M.G., Xia H. and Yokoyama M. 2006 *Plasma Phys. Control. Fusion* **48** S17
[29] Fujisawa A. *et al* 2006 *Plasma Phys. Control. Fusion* **48** S31
[30] Watari T., Hamada Y., Fujisawa A., Toi K. and Itoh K. 2005 *Phys. Plasmas* **12** 062304
[31] Itoh K., Itoh S.-I., Diamond P.H., Fujisawa A., Yagi M., Watari T., Nagashima Y. and Fukuyama A. 2006 *Plasma Fusion Res.* **1** 037
[32] Gao Z., Itoh K., Sanuki H. and Dong J.Q. 2006 *Phys. Plasmas* **13** 100702
[33] Hidalgo C. *et al* 1999 *Phys. Rev. Lett.* **83** 2203
[34] Hidalgo C. *et al* 2006 *Plasma Phys. Control. Fusion* **48** S169
[35] Xu Y.H. *et al* 2000 *Phys. Rev. Lett.* **84** 3867
[36] Diamond P.H. *et al* 1994 *Phys. Rev. Lett.* **72** 2565

[37] Goncalves B., Hidalgo C., Pedrosa M.A., Orozco R.O., Sanchez E. and Silva C. 2006 *Phys. Rev. Lett.* **96** 145001
[38] Kim Y.C. and Powers E.J. 1979 *IEEE Trans. Plasma. Sci.* **PS-7** 120
[39] Tynan G.R., Moyer R.A., Burin M.J. and Holland C. 2001 *Phys. Plasmas* **8** 2691
[40] Burin M.J., Tynan G.R., Antar G.Y., Crocker N.A. and Holland C. 2005 *Phys. Plasmas* **12** 052320
[41] Nagashima Y. *et al* 2005 *Phys. Rev. Lett.* **95** 095002
[42] Itoh K. *et al* 2005 *Phys. Plasmas* **12** 102301
[43] Ritz Ch.P., Powers E.J. and Bengston R.D. 1989 *Phys. Fluids* B **1** 153
[44] Crossley F.J. *et al* 1992 *Plasma Phys. Control. Fusion* **34** 235
[45] Xia H. and Shats M.G. 2003 *Phys. Rev. Lett.* **91** 155001
[46] Fujisawa A. *et al* 2006 *Plasma Phys. Control. Fusion* **48** A365
[47] Fujisawa A. *et al* 2006 *Plasma Phys. Control. Fusion* **48** S205
[48] Shats M., Solomon W.M. and Xia H. 2003 *Phys. Rev. Lett.* **90** 125002
[49] Hamada Y. *et al* 2006 *Phys. Rev. Lett.* **96** 115003
[50] Melnikov A.V. *et al* 2003 *Proc. 30th EPS Conf. on Controlled Fusion and Plasma Physics (St Petersburg, Russia, 2003)* vol 27A (ECA) P-3.114